ASSESSMENT OF EXISTING FORMULAS FOR EQUIVALENT DAMPING TO USE IN DIRECT DISPLACEMENT-BASED DESIGN

H. Degée[1] , R. Bento[2] and B. Massena[3]

[1] *Research Associate, Dept. ArGenCo, University of Liège. Belgium*
[2] *Associate Professor, ICIST, IST, Lisbon, Portugal*
[3] *PhD Student, ICIST,IST, Lisbon, Portugal*
Email: H.Degee@ulg.ac.be

ABSTRACT :

It is generally stated that an accurate evaluation of the equivalent viscous damping is a crucial step in the Direct Displacement-Based Design (DDBD) methodology. A wrong assessment of equivalent viscous damping can indeed lead to important errors on the actual ductility demand of the structural elements. The objective of the present contribution is to assess and compare different existing formulas for the evaluation of the equivalent damping and to provide information on the impact of choosing one or another formulation on the seismic design. It is more precisely focused on the very recent proposals of Dwairi – Kowalsky and Blandon – Priestley.

KEYWORDS: Direct Displacement-Based Design, Reinforced Concrete Structures, Equivalent Viscous Damping

1. INTRODUCTION

Even if methodologies based on forces are still the most widespread in various design codes to estimate the response of structures subjected to seismic action, a growing interest appeared during the last years for methods based on displacements, in particular for what regards reinforced concrete structures, as they are felt more appropriate and able to overcome inherent deficiencies of traditional force-based methodologies. One of the new design procedures is the Direct Displacement-Based Design (DDBD) initiated by Priestley [1, 2]. In this approach, structures are designed in order to achieve displacements corresponding to a specified limit state, rather than to be limited by such displacements. In DDBD, the non-linear structure is represented by an equivalent SDOF system characterized by the secant stiffness associated with the maximum displacement and by a level of equivalent viscous damping ξ_{eq} representing the combined effect of viscous and hysteretic dissipation.

The estimation of the equivalent viscous damping is a crucial point of the DDBD methodology. In this context, the main objective of this work is to assess and compare different existing equations aiming at evaluating the equivalent damping and to provide information on the practical consequences of choosing one or another of these equations in the design process. The paper presents a summary of results obtained from different investigations about the equivalent viscous damping for use in the DDBD methodology. After a comprehensive inventory of the equations available in the literature to correlate the effective period, the design ductility and the equivalent viscous damping, a comparison is performed between the equivalent viscous damping obtained from numerical non-linear time-history analyses for different types of ground motion and the equivalent damping obtained with the two most recent theoretical formulations. The second part of the paper investigates the consequences of choosing one or another damping equation on the design process.

Figure 1 presents the equivalent damping obtained with some of the most recent formulas summarized in Table 1. Table 1 provides also information on the ground motion database used in the calibration procedure. The obtained values exhibit a rather important scattering with differences up to 50% in some cases. Furthermore, even if most authors are stating that the type of ground motion may have an influence, none of the proposed expression includes the effect of this parameter.

Table 1 – Existing equivalent viscous damping equations

Author	Proposed equations	Hysteretic model	Ground motion
Priestley (2003) [3]	$\xi_{eq} = \xi_0 + \frac{120}{\pi}\left(1 - \frac{1}{\sqrt{\mu}}\right)\%$	Takeda model, large cycles (concrete beams and frames)	Sinusoidal motion
	$\xi_{eq} = \xi_0 + \frac{95}{\pi}\left(1 - \frac{1}{\sqrt{\mu}}\right)\%$	Takeda model, narrow cycles (concrete columns and walls)	
	$\xi_{eq} = \xi_0 + \frac{25}{\pi}\left(1 - \frac{1}{\sqrt{\mu}}\right)\%$	Precast walls or frames, with unbounded prestressing	
	$\xi_{eq} = \xi_0 + \frac{150}{\pi}(\mu - 1)\%$	Elasto-Plastic behavior (for steel members)	
Kwan (2003) [4]	$\xi_{eq} = \frac{2C_2}{\pi}\left(0.8\mu^{C_1}\right)^2 \frac{\mu - 1}{\mu^2} + 0.55\left(0.8\mu^{C_1}\right)^2 \xi_0$	- Elasto-plastic - Slightly and moderately degrading systems - Bilinear hyper-elastic	20 artificial ground motions
Blandon (2004) [5]	$\xi_{eq} = \xi_0 + \frac{a}{\pi}\left(1 - \frac{1}{\mu^b}\right)\left(1 + \frac{1}{(T_{eff} + c)^d}\right)\frac{1}{N}$ $N = 1 + \frac{1}{(0.5 + c)^d}$	- Narrow Takeda model - Large Takeda model - Elasto-plastic - Bilinear hyper-elastic - Ramberg-Osgood - Ring spring	5 artificial records and 1 real record
Dwairi et al.(2007) [6]	$\xi_{eq} = \xi_0 + C_{RS}\left(\frac{\mu - 1}{\pi\mu}\right)\%$ $C_{RS} = 30 + 35(1 - T_{eff})$ $T_{eff} < 1\text{sec}$ $C_{RS} = 30$ $T_{eff} \geq 1\text{sec}$	- Ring Spring	100 ground motions
	$\xi_{eq} = \xi_0 + C_{LT}\left(\frac{\mu - 1}{\pi\mu}\right)\%$ $C_{LT} = 65 + 50(1 - T_{eff})$ $T_{eff} < 1\text{sec}$ $C_{LT} = 65$ $T_{eff} \geq 1\text{sec}$	- Large Takeda model	
	$\xi_{eq} = \xi_0 + C_{ST}\left(\frac{\mu - 1}{\pi\mu}\right)\%$ $C_{ST} = 50 + 40(1 - T_{eff})$ $T_{eff} < 1\text{sec}$ $C_{ST} = 50$ $T_{eff} \geq 1\text{sec}$	- Narrow Takeda model	
	$\xi_{eq} = \xi_0 + C_{EP}\left(\frac{\mu - 1}{\pi\mu}\right)\%$ $C_{EP} = 85 + 60(1 - T_{eff})$ $T_{eff} < 1\text{sec}$ $C_{EP} = 85$ $T_{eff} \geq 1\text{sec}$	- Elasto-Plastic	

ξ_0 - initial viscous damping

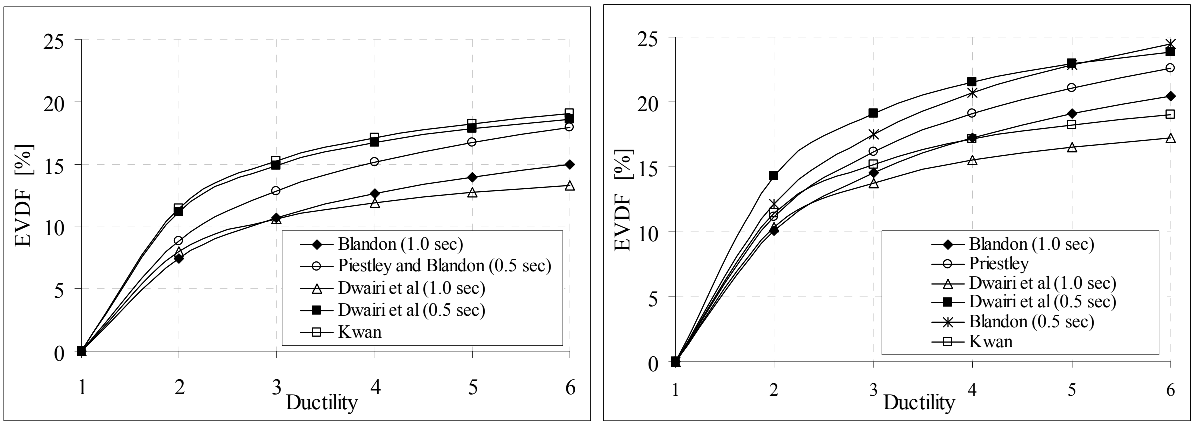

Figure 1 Comparison of Equivalent Viscous Damping Factor
a) Narrow Takeda model - b) Large Takeda model

2. Assessment of existing formula

As referred, the main objective of the equivalent damping concept is to allow the definition of an easy and reliable relation between the maximum displacement of the inelastic system and its effective period, assuming a given ductility level. Therefore, in order to be used for comparison and assessment purposes, a full set of SDOF systems are defined, for which the effective period, the maximum displacement and the ductility level are known and consistent. The main governing parameters of these simple systems are given on Fig. 2. As the focus is essentially on the hysteretic behavior, the viscous damping ξ_0 is assumed equal to zero.

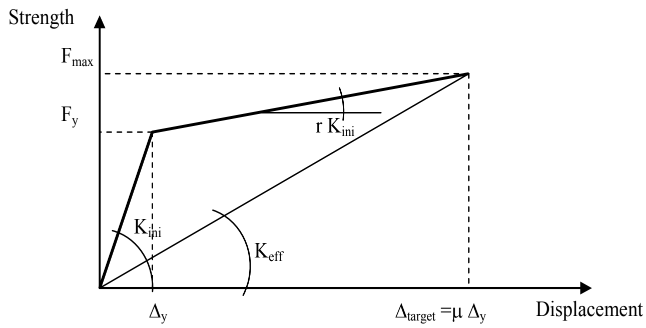

$$K_{eff} = \frac{4\pi^2 m_{eff}}{T_{eff}^{\ 2}}$$

Figure 2 Constitutive law of the SDOF system

T_{eff} is the effective period of the system, μ is the assumed ductility, m_{eff} is the effective mass (assumed constant for all considered cases) and K_{eff} the effective stiffness. The parameters of the different considered SDOF systems are calibrated in such a way that the average of the maximum displacement obtained by non-linear time-history analyses is equal to the target displacement Δ_{target} of Fig. 2.

Six groups of SDOF systems are defined according to the type of assumed hysteretic behavior (large or narrow Takeda model) and to the type of ground motion time-history. The narrow Takeda model (α = 0.5 and β = 0) is generally assumed suitable for columns and walls and the large Takeda model (α = 0.3 and β = 0.6) for reinforced concrete beams and frames [7].

Three series of ground motions are considered:
1. The first series (Series 1) is a set of 10 accelerograms including the 5 synthetic accelerograms used by Blandon and Priestley for the calibration of their equivalent damping formula [6] and five new generated accelerograms. These accelerograms correspond to a reference displacement spectrum more or less linear up to a corner period equal to 4s, with a PGA equal to 0.7g.

2. The second series is a set of 10 artificially generated accelerograms with a spectrum compatible with a type 1 spectrum of Eurocode 8, with a PGA equal to 0.7g.
3. The third series is a set of 10 artificially generated accelerograms with a spectrum compatible with a type 2 spectrum of Eurocode 8, with a PGA equal to 0.5g.
Figure 3 represents, for each of the three series, the reference spectrum (i.e. a linear function of the effective period up to the corner period T_c) and the average spectrum obtained from the selected accelerograms for a viscous damping of 5%. Accelerograms of series 2 and 3 were generated with the GOSCA software [8].

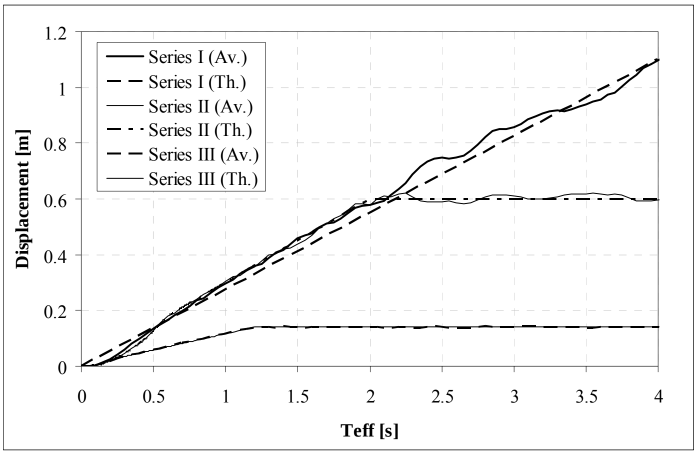

Figure 3 Reference displacement spectrum (Th.) and average numerical spectrum (Av.) for each series

As a matter of example, Figure 4 presents the target displacement obtained for effective periods ranging from 0.5s to 3.5s and ductility ranging from 2 to 6 with the first series of accelerograms, respectively for narrow and large Takeda hysteretic model. The curves plotted on these figures can be considered as inelastic displacement spectrum expressed as a function of the effective period, i.e. associated with the period related to the secant stiffness corresponding to the maximum expected displacement. Figure 4 show a general trend to decreasing displacements when the ductility increases, due to a greater amount of energy dissipated in the hysteretic cycles. Further, for similar effective period and ductility, the maximum displacement obtained with the large Takeda model is smaller than the one obtained with the narrow Takeda model, which is again due to the greater amount of energy dissipated in the former model. The whole set of results obtained for the 3 series can be found in Ref. [7].

From these numerical displacements, it is then possible to evaluate an equivalent viscous damping level for each configuration (i.e. for each couple T_{eff} - μ). This is done numerically by computing, by means of linear time-history analyses, the average elastic displacement spectrum for each series of ground motion and for different level of viscous damping, and by selecting the viscous damping level that provides an average spectral displacement equal to the maximum displacement of the NLTHA. The period of the SDOF system is the effective period of the studied configuration.

The whole set of results (available in [7]) can then be used to assess the recent proposals of Blandon – Priestley (B-P) and Dwairi – Kowalsky (D-K). Figure 5 compares the relative difference between the values of equivalent damping. An exhaustive comparison is done for both narrow and large Takeda hysteretic models and for the 3 series of ground motion in Ref. [7]. Even if it is difficult to draw general conclusions from such a small sample of ground motion, some general tendencies can however be observed:
- The average relative error between numerical results on one hand and approximated results (B-P and D-K) on the other hand tends to diminish when ductility increases. This means also that damping tends towards underestimated values for higher ductility level.
- A slight tendency to a decreasing error can be observed when effective period increases.
- For low ductility level, B-P approach leads to higher values of damping than D-K approach, while the tendency is inverted for high ductility level.

- Except for very short effective periods (≤ 0.5s), for periods greater than the corner period and for some specific cases of low ductility, the absolute value of the relative error between numerical results and results obtained from the formulas is always under 25%.

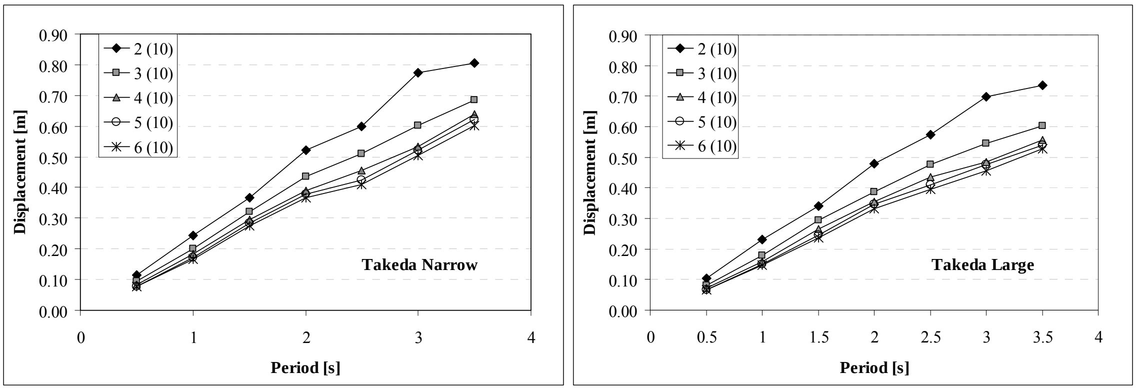

Figure 4 Target displacement as a function of the effective period for different ductility level (1st series)

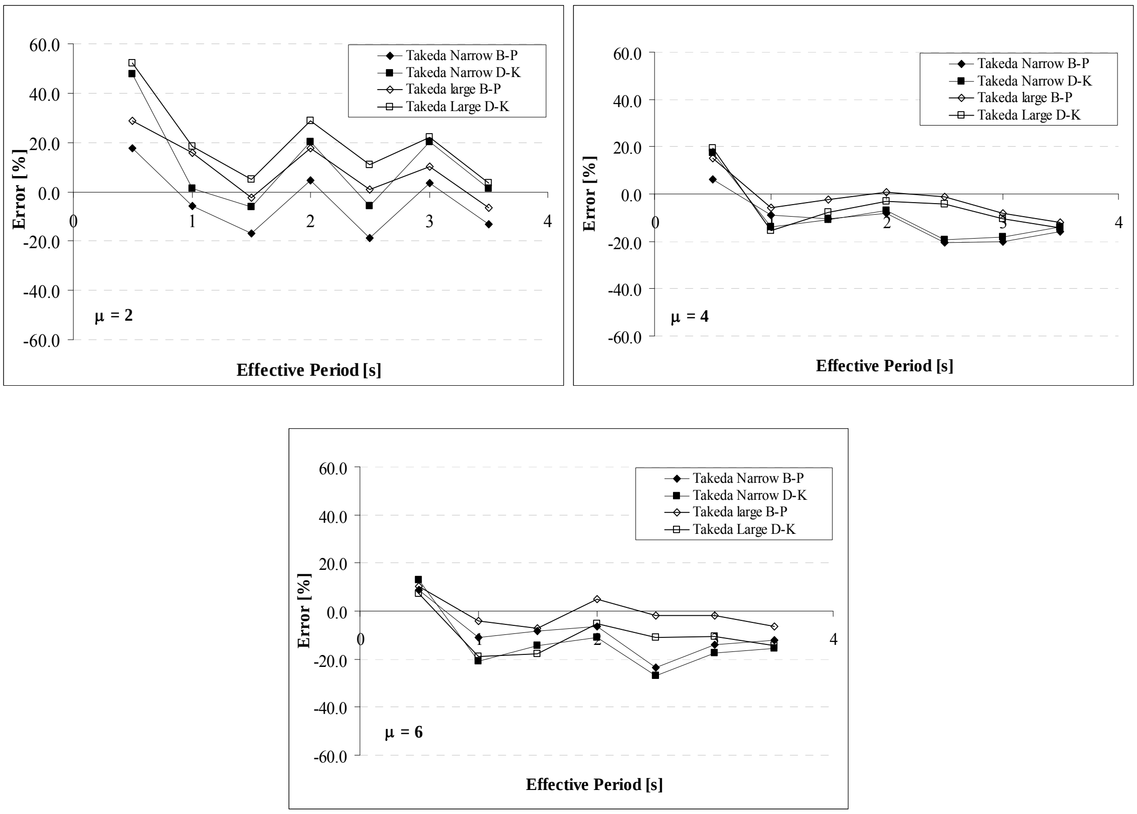

Figure 5 Relative error on the damping [$(ED_{formula}-ED_{num})/ED_{num}$ in %] (1st Series)

3. ASSESSEMENT OF THE DESIGN USING EQUIVALENT VISCOUS DAMPING

In the previous section of the paper, the methods have been compared essentially on the base of the provided equivalent damping values referred to values obtained through NLTHA. However, in the DDBD context, this equivalent damping is not the final objective, but only a tool to define the characteristics of the designed system (effective period, stiffness, base shear) for a given value of the target displacement. In order to study the problem from this reverted point of view, an example of design of a single circular bridge pile adapted from Priestley [3] is used (see Figure 6 and Ref. [7]). The designed pile is then subjected to a series of NLTHA and the ductility assumed for the design is compared to the actual ductility demand.

The yield displacement Δ_y of the pile is given by Eq. (3.1). No drift limit is considered in the design, in order to allow for any ductility without being limited by the overall rotation of the system.

$$\Delta_y = 2.35\varepsilon_y H^2 / 3d \qquad (3.1)$$

Three design situations were considered:

- **Case 1**: design on the base of the theoretical spectrum (i.e. a linear function of the effective period, see also Fig. 3) corresponding to the first series of accelerograms considered in the previous section of the paper (Series 1), assuming a narrow Takeda hysteretic behavior of the pile, which is the one recommended for columns;
- **Case 2**: design on the base of the average spectrum computed from the full 1st series of accelerograms, with a narrow Takeda hysteretic behavior. In this case, the only source of difference between the assumed ductility and the actual ductility of the system would only be the coarse estimation of the equivalent damping, while in case 1, an other possible source is the difference between the theoretical spectrum used for the design and the actual spectrum corresponding to the accelerograms used for the assessment;
- **Case 3**: design on the base of the theoretical spectrum corresponding to the first series of accelerograms, but assuming a large Takeda hysteretic behavior, which is less realistic for a pile, but allows an assessment of the consequences of an improper choice as regards the type of dissipative behavior.

The diameter and height of the pile are defined in order to target specific values of the effective period and of the design ductility, even if some of the resulting configurations may not be very representative of practical situations. The design is performed according to the formulas proposed by Priestley [3], Blandon – Priestley [5] and Dwairi – Kowalsky [6] and the resulting effective period for each situation are presented in Table 2. In all cases, Priestley formula (derived on the base of sinusoidal ground motion) leads to higher effective periods than the other two formulas and, in general, B-P and D-K approaches lead to very close values of the effective period, except for low ductility level, where D-K approach produces slightly higher values. It is also interesting to stress that, when the effective period is higher, the effective stiffness and hence the design base shear are decreasing consequently.

The resulting SDOF systems are submitted to the accelerograms of the first series. In order to assess B-P and D-K equations, Table 3 presents three different procedures for comparing the actual ductility demands. Firstly it compares the actual ductility demands obtained for systems designed for the same design conditions (case 1 and case 2 respectively) but using either B-P or D-K equation for the estimation of the equivalent damping. Secondly it compares the actual ductility demands obtained with the same equivalent damping definition (B-P and D-K respectively) but with a displacement spectrum being either the theoretical one or the exact spectrum obtained for the selected accelerograms used for the NLTHA assessment. Finally the third one compares the actual ductility demands obtained with the same equivalent damping definition (B-P and D-K respectively) but corresponding to different hysteretic models (narrow or large Takeda).

The main outcome of this comparison is that the average difference resulting from the choice of either B-P or D-K equation, and even from the choice of either a narrow or a large Takeda hysteretic model, is smaller than the average difference resulting from the use of either a theoretical spectrum or a real one.

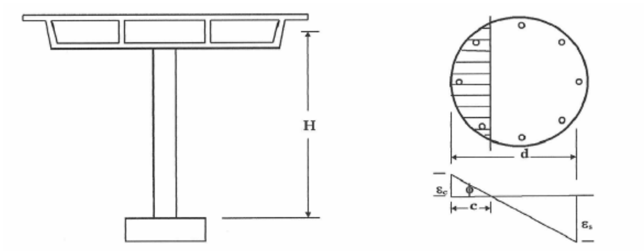

Figure 6 Typical geometry of the example (single pile)
(a) Cantilever Bridge columns (b) Column section and Limit State Strains

Table 2 Effective period obtained for the different configurations

Case 1 (Takeda narrow – design spectrum)			Case 2 (Takeda narrow – numerical spectrum)			Case 3 (Takeda large – design spectrum)		
T_{eff} [s] Priestley	T_{eff} [s] Blandon-Priestley	T_{eff} [s] Dwairi-Kowalsky	T_{eff} [s] Priestley	T_{eff} [s] Blandon-Priestley	T_{eff} [s] Dwairi-Kowalsky	T_{eff} [s] Priestley	T_{eff} [s] Blandon-Priestley	T_{eff} [s] Dwairi-Kowalsky
1.04	0.98	1.00	0.98	0.93	0.96	1.12	1.08	1.09
1.01	0.95	0.92	1.02	0.96	0.95	1.10	1.05	1.02
1.00	0.94	0.89	1.04	0.97	0.94	1.10	1.05	0.96
2.00	1.86	1.94	1.81	1.67	1.75	2.17	2.04	1.97
1.98	1.81	1.81	1.92	1.72	1.74	2.16	2.03	2.00
2.02	1.84	1.81	2.18	1.78	1.74	2.22	2.08	2.00
3.02	2.80	2.94	3.47	2.74	3.00	3.55	3.34	3.45
3.00	2.74	2.76	3.38	2.77	2.71	3.29	3.07	3.03
3.00	2.74	2.78	3.42	2.80	2.71	3.30	3.07	2.96

Table 3 Relative difference on the actual ductility demand between (i) B-P and D-K for a same design case, (ii) Case 1 and Case 2 for a same approach, (iii) Case 1 and Case 3 for a same approach [in %]

	B-P / D-K		Case 1 / case 2		Case 1 / Case 3	
Configuration	Case 1	Case 2	B-P	D-K	B-P	D-K
1	-0.1	0.1	4.5	4.8	-2.3	-4.5
2	5.5	2.9	-2.9	-5.4	-0.9	2.0
3	12.2	0.1	-0.8	-11.5	1.9	7.3
4	-7.2	-10.6	12.9	8.8	4.9	15.3
5	-0.2	-2.0	7.2	5.3	-4.5	-0.8
6	4.4	1.5	8.2	5.3	-5.7	3.4
7	-7.1	-11.8	7.8	2.3	-1.9	-3.3
8	0.4	13.5	0.5	13.7	0.1	-1.3
9	0.3	4.1	-3.2	0.5	-0.7	5.8
average	***0.9***	***-0.2***	***3.8***	***2.6***	***-1.0***	***2.6***

4. CONCLUSION

This paper has presented a summary of results obtained from different investigations about the equivalent viscous damping for use in the Direct Displacement-Based methodology. After a comprehensive inventory of the most recent equations available in the literature to correlate the effective period, the design ductility and the equivalent damping, a comparison was performed between the equivalent damping obtained from numerical NLTHA for different types of ground motion and the equivalent damping obtained with the two most recent theoretical formulations proposed respectively by Blandon-Priestley and Dwairi-Kowalsky. The main outcome of this comparison is that, except in some specific conditions that should require additional investigations (i.e. very small effective periods, effective periods greater than the corner period of the displacement spectrum and some cases of low ductility), the different approaches lead to a rather important scattering of the results, but with a range of variation of the error between the damping values obtained from numerical and theoretical approaches smaller than 25%.

The second part of the paper aimed at investigating the consequences of the choice of one or another damping equation on the design. It comes to the conclusion that both Blandon-Priestley and Dwairi-Kowalsky approaches lead to an accurate design for small ductility and to a safe design, even if less accurate, for moderate to high assumed ductility. Further it appears impossible to determine if one of the two approaches is better than the other, as the difference in terms of accuracy related to the assumed shape of the design spectrum is greater than the difference related to the choice of one or another viscous damping formulation.

5. ACKNOWLEDGEMENTS

This work is part of the research activity carried out at ICIST and has been partially supported by FEDER and FCT through project POCI/ECM/59306/2004. H. Degée thanks for the support received from F.R.S.-FNRS (Belgian Fund for Research). Part of this work is also included in the working plan of the PhD student B. Massena financial supported by FCT (SFRH/BD/36648/2007).

REFERENCES

[1] Priestley, M.J.N. (1993). Myths and Fallacies in Earthquake Engineering - conflicts between design and reality. *Bulletin of the New Zealand National Society for Earthquake Engineering* **Vol. 26:3**, 329–341.
[2] Priestley, M.J.N. and Kowalsky, M.J. (2000). Direct Displacement-Based Seismic Design of Concrete Buildings. *Bulletin of the New Zealand National Society for Earthquake Engineering* **Vol. 44:2**, 145–165.
[3] Priestley, M.J.N. (2003). Myths and Fallacies in Earthquake Engineering, Revisited. The Mallet Milne Lecture, IUSS Press, Pavia, Italy.
[4] Kwan W.P. and Billington S.L. (2003) Influence of hysteretic behavior on equivalent period and damping of structural systems. *ASCE Journal of Structural Engineering* **129:5**, 576-585.
[5] Blandon, C.A. and Priestley M.J.N. (2005) Equivalent viscous damping equations for direct displacement design. *Journal of earthquake Engineering,* **No 9 (special issue 2)**, 257-278.
[6] Dwairi, H.M. and Kowalsky, M.J. (2004). Investigation of Jacobsen's Equivalent Viscous Damping Approach as applied to Displacement-Based Seismic Design. *13th World Conference on Earthquake Engineering – 13WCEE.* **Paper No 228,** Aug. 1-6, Vancouver, Canada.
[7] Degée, H., Bento, R. and Massena, B. (2007). Complementary Investigation on the Equivalent Viscous Damping in Direct Displacement-Based Design, ICIST Research Report DTC nº 11/07, IST Lisbon (Portugal).
[8] Denoel, V. (2001) Generation of Spectrum Compatible Accelerograms, Research Report, Université de Liège, Belgique.